Submitted to Chem Rev Soc – revised version September 20, 2013

TUTORIAL REVIEW

1D oxide nanostructures from chemical solutions

Mari-Ann Einarsrud and Tor Grande

Department of Materials Science and Engineering, Norwegian University of Science and Technology, NO-7491 Trondheim, Norway

Abstract

Nanotechnology has motivated a tremendous effort to grow free standing or hierarchical nanomaterials such as nanowires and nanorods. Bottom-up approaches based on chemistry are an important approach to nanomaterials, and here the concepts of growing oxide 1D nanostructures from chemical solutions are reviewed. The thermodynamic and kinetic aspects of the nucleation and growth of oxide in solutions are presented with emphasis on hydrothermal and molten salt synthesis. The importance of solubility of precursors, the precursor chemistry, role of organic additives as well as the chemical complexity and dimensionality and symmetry of the crystal structure of the compound grown are highlighted.

Key learning points

In this tutorial review, a critical overview is proposed to the reader, providing fundamental knowledge about:

(1) How to develop new synthesis routes to 1D oxide nanostructures from chemical solutions
(2) The basic mechanisms for unidirectional growth of oxide materials from chemical solutions
(3) The chemical, physical and structural aspects important for synthesis of 1D oxide nanostructures from chemical solutions
(4) The principles and the formation mechanisms of 1D oxide nanostructures using the hydrothermal synthesis
(5) The principles of the molten salt route to 1D oxide nanostructures

1. Introduction

Nanostructured materials, possessing at least one dimension between 1 and 100 nm, have received considerable attention in recent years. Nanowires, nanorods and whiskers constitute the class of nanocrystalline materials termed one dimensional (1D) nanostructures due to the elongation of the extension of the structure in one specific direction. 1D nanostructures are thereby distinguished from more frequent nanoparticles (0D) and thin films (2D). The prospects of utilizing 1D nanostructures has been reported in many different applications such as non-volatile ferroelectric random access memories, nano-electromechanical systems, energy-harvesting devices, advanced sensors and in photocatalysis.[1-4] The 1D nanostructures can be used as interconnects and functional units in these applications as well as opening up for novel sophisticated nanoarchitectures. Anisometric particles can also be used in composites for improving the mechanical performance, for example in nanocomposites combining the unique properties of soft and hard materials. From a more fundamental point of view nanostructures also attract attention due finite size effects and possible new physical phenomena emerging due to downscaling.[5] In this context 1D nanostructures provide excellent model systems to study the dependence of transport of charge, spin and heat on dimensionality and size.[1] This is particularly interesting for materials with anisotropic crystal structures, where anisotropic properties may be enhanced or depressed depending on the crystallographic direction of the 1D nanostructures. 1D nanostructures are also attractive for fundamental studies of mechanical properties and finite size.

Physical or chemical deposition methods have been very successful in fabrication of semiconducting nanowires and hierarchical structures of these.[3,6] Nanostructures of simple oxides such as ZnO can also be prepared by such routes, while routes to more complex oxides such as perovskite materials cannot easily be adopted by these deposition techniques.[7] 1D oxide nanostructures can more easily be prepared from solution based synthesis routes, which opens up for a rich variety of precursor chemistry, solvents and the use of organic additives like surfactants to guide the crystal growth,[8,9] and hydrothermal or solvothermal synthesis have shown great promise in preparation of 1D oxide nanostructures.[10,11] Solvents stable at higher temperatures with higher solubility of the principle oxides have also been used such as molten salts.[12] The literature concerning these synthesis methods is most often focused on reporting successful synthesis protocols and is to a large degree empirical in nature. Unfortunately, the reproducibility of some of these routes are not always impressive,[13] and it can be challenging to find useful guidelines to design a new synthesis pathway without previous experience of using chemical routes to nanomaterials.

Here, we present a tutorial review on the synthesis and growth of 1D oxide nanomaterials from chemical solutions. We will focus on using the hydrothermal synthesis route, where essentially water is the solvent and the molten salt method, where higher temperatures are accessible with higher solubility of the principle oxides. Critical thermodynamic and kinetic aspects of the synthesis routes will be addressed as well as the important role of the complexity of the compounds with respect to chemistry and crystal structure.

2. Principles for solution based synthesis of 1D oxide nanostructures

Solution based chemical syntheses are well-established routes to inorganic materials in general.[14] Solution-based methodologies of material synthesis offer several advantages with respect to flexibility, environmental friendliness and simplicity compared to top-down-based preparation techniques such as lithographic methods. The flexibility stems from the fact that a wide range of chemical precursors can be used as well as several different types of solvents. From an environmental point of view water is the preferred solvent to be used. Flexibility is also connected to the possibility to change the synthesis parameters like concentration, reaction time, temperature, pH, additives, stirring rate and atmosphere. Organic additives acting as complexing agents can also be utilized to increase the solubility and stability of the chemical solutions. Syntheses from chemical solutions include precipitation, sol-gel-based methods, hydrothermal synthesis, combustion synthesis, molten salt method and spray pyrolysis among others.

These solution based synthesis routes in its simple form like standard sol-gel method have several limitations with respect to prepare 1D oxide nanostructures, and it might be a challenge to grow most materials into 1D shape without additional adjustments. There are however some exceptions as illustrated here by the formation of single-crystal lanthanide orthophosphate 1D nanowires by a simple hydrothermal synthesis.[15] Fang et al. were able to grow the hexagonal polymorph of these materials (*e.g.* $LaPO_4$) because it has an anisotropic crystal structure which facilitate the crystal growth along the c-direction. On the contrary, tetragonal lanthanide orthophosphate materials (*e.g.*YPO_4) have no preferred growth direction based on the crystal structure and only spherical nanoparticles were formed.[15] Hence a shape directing approach is normally necessary to grow 1D nanostructures if the crystal structure of the targeted oxide does not have an anisotropic crystal structure which easily grows in one crystallographic direction.

Different approaches have therefore been proposed to achieve 1D growth by solution based synthesis.[1,7] These approaches include a) use a precursor with 1D nanostructure, b) apply appropriate organic additives or surfactants to aid directed growth, c) oriented attachment of non-spherical nanocrystals into 1D nanostructures, d) confinement by a hard template with 1D morphology or e) confinement by a liquid drop. Here we will focus on the approaches a), b) and c) which all can be taken advantage of in a solution based synthesis of single crystalline oxide materials. In addition we will focus on the synthesis of materials with anisotropic crystal structures which easily grow in one crystallographic direction. Approach d) can only be used to make polycrystalline 1D nanostructures while e) is mostly used for semiconductors such as Si, GaAs and ZnO.[6]

In the following we will explain how we can apply these approaches in hydrothermal or molten salt synthesis to prepare 1D oxide nanostructures. We will also explain or advice how these syntheses should be performed. Complex oxides like perovskites are especially challenging to prepare into 1D nanostructures and it might also be challenging to prepare stable aqueous or non-aqueous solutions containing all the necessary precursors to obtain the

desired product. To increase the solubility of the precursors, hydrothermal and molten salt syntheses approaches are especially advantageous.

3. Hydrothermal synthesis of 1D oxide nanostructures

Definition of hydrothermal reaction: Heterogeneous chemical reaction in aqueous media above room temperature (normally above 100 °C) and at a pressure greater than 1 atm.[16, 17]

Hydrothermal synthesis involves heating the chemical solution in a sealed vessel (autoclave) which thereby increases the autogeneous pressure inside the vessel beyond atmospheric pressure as the temperature exceeds the boiling point of the solvent. This will provide increased solubility and reactivity of the precursors used in the material synthesis. If water is used as the solvent, the process is called hydrothermal[16, 17] while in the case of a non-aqueous solvent the process is termed solvothermal.[18] Here we will mainly focus on hydrothermal processes.

3.1 Principles of hydrothermal synthesis

During hydrothermal synthesis, the properties of water are changing (*e.g.* density, ionic product, viscosity and dielectric constant) with increasing temperature and pressure.[19] The density, dielectric constant and ionic product, K_w, of water at 30 MPa as a function of temperature is illustrated in Fig. 1. As the temperature increases, the density of water decreases while the density of the gas phase (steam) increases. At the critical point, the densities of both phases are equal and the difference between the liquid and the gas has disappeared. Above the critical point (374 °C, 218 atm) only the supercritical fluid exists. The dielectric constant of water drops drastically as water is heated and approaches the properties of non-polar solvents at supercritical conditions, hence this will influence on the solubility of the precursors as non-polar precursors will be more soluble.

The pressure-temperature diagram of water is given in Fig. 2 for different filling factors of the autoclave. The figure illustrates how important the filling factor of the autoclave is for the pressure generated. The stippled curve up the critical temperature represents the line where the liquid water and the gaseous phase coexist. Below this curve, liquid water is not present and the vapor phase is not saturated. Above this curve, the system consists only of compressed liquid water. The pressure inside the vessel partially filled with water is illustrated in the figure with the solid lines. Filling the autoclave to more than 32 %, for example 70 %, the vessel is completely filled with liquid water at a temperature of about 300 °C. Increasing the temperature further will increase the pressure inside the autoclave according to the 70 % line. Using a filling factor lower than 32 %, the liquid water-gas

interface inside the autoclave will be lowered and at a certain temperature the autoclave will be completely filled with only the gas phase.

We should keep in mind that Figs. 1 and 2 only specify the properties of pure water. The precursors, used during the hydrothermal reactions will influence on the composition of both the liquid and gas phase, which naturally will change the pressure-temperature profile of the liquid-gas equilibrium in the autoclave during the hydrothermal synthesis. The pressure will be lowered from that of pure water by the presence of the dissolved ions in the aqueous solution. On the contrary precursors which will decompose at the given temperature will cause the pressure to increase due to the generation of gases during decomposition of for example complex anions, i.e. nitrates, carbonates decomposing to nitrous gases or CO_2.

Some syntheses performed hydrothermally include water in the supercritical state.[20] However, in most hydrothermal syntheses the temperature and the pressure are kept below the critical point. These syntheses are therefore performed under mild hydrothermal conditions, but we still take advantage of the higher reactivity and increased solubility of the precursors without taking the water to the supercritical state.

3.2 Mechanisms for growth of 1D nanostructures by hydrothermal method

The most probable mechanism for nucleation and growth of oxide materials during hydrothermal synthesis is dissolution/reprecipitation, which include dissolution of precursors, diffusion of dissolved precursor species and precipitation/reaction to give the targeted compound. This growth mechanism can explain the growth of 1D nanostructured materials with anisotropic crystal structures, when appropriate organic additives or surfactants to aid directed growth are used or by use of oriented attachment of non-spherical nanocrystals into 1D nanostructures. The dissolution is enhanced by the hydrothermal conditions, while the diffusivity of the dissolved species is increased by the reduced viscosity of the water at hydrothermal conditions. The solubility of the precursors is of great importance for this mechanism, and hence understanding of the complex solution chemistry is necessary. If a highly anisotropic crystal structure of an intermediate compound is transformed to the target oxide a complete solubilization, at the least at the initial state of the synthesis at least, is not desired. Otherwise it is difficult to see how the product material could mirror the precursor shape and in this case a topotactic mechanism is the most probable. In a topotactic reaction the atomic arrangement on the reactant crystal remains largely unaffected during the course of the reaction while changes in the dimensions can occur. Several other growth mechanisms than dissolution/reprecipitation are also discussed in literature and we will discuss reaction mechanisms further in the examples given in Chapter 3.4.

The solubility of the precursors might still not be sufficient to give high enough diffusion of the dissolved species for an efficient synthesis. Often a mineralizer has to be added to increase the solubility. Hence the function of the mineralizer is to increase the solubility of the precursors. To choose the optimal mineralizer we have to consider the chemistry of the oxide and precursors species we want to dissolve. For example increased solubility of

amphoteric and acidic oxides can be obtained by using basic mineralizers (*e.g.* NaOH or KOH). Basic oxides often have a high solubility at the hydrothermal synthesis conditions. In addition, different salts and organic additives like complexing agents are commonly used as mineralizers especially for larger metal cations to enhance solubility.[21] Examples here are the use of EDTA for the formation of PZT and the use of citric acid to overcome the problem of differing solubilities between different cations.[21]

3.3 How to perform the hydrothermal synthesis?

The hydrothermal synthesis is performed by placing the selected precursors, mineralizer and additives together with the solvent (normally water) in the autoclave as illustrated in Fig. 3. Normally steel autoclaves with a Teflon® lining to avoid contamination from the steel are used. A filling factor sufficient to give the necessary pressure is used (normally filling factors below 80 % are used). For most hydrothermal syntheses only moderate temperatures between 100 and 300 °C are applied meaning that the hydrothermal conditions are below the supercritical region. The precursors are normally not dissolved in the water at room temperature and the feed solution is a suspension or amorphous precipitates are formed adding the basic mineralizer. Precursors can be oxides, hydroxides, or salts of the elements to build up the material. The autoclave is heated either by placing it in an oven or by using microwaves. The phase composition and morphology of the product can be governed by even small changes in the chemical parameters like the type of precursors, concentration, pH as well as the process parameters like reaction time and temperature.[10] At the present stage of understanding of hydrothermal synthesis of 1D nanostructures it is difficult to predict the effect of the chosen reaction parameters. Many syntheses are based on the trial and error principle rather than a designed synthesis approach. The following tools are developed/used to approach a rational materials design using hydrothermal synthesis and to figure out the preferred synthesis conditions:

- Thermodynamic calculations of phase equilibria to aid in the determination of the parameter space which will give the targeted phase.[21, 22]
- To speed up the process, combinatorial synthesis can be performed by placing several sealed Teflon® bags with reaction media varying one specific parameter (e.g. pH) into the same steel autoclave. By a combinatorial synthesis approach we can scan a large parameter space within a reasonable time frame.[23]
- The application of *in-situ* characterization techniques to study the reaction intermediates and reaction mechanisms.[24]

Normally, reaction times from hours to several days are necessary. After cooling of the autoclave, the product is separated by filtration and further washed in several washing steps. Continuous hydrothermal synthesis has also been developed for nanoparticles.[25]

3.4 Hydrothermal growth of 1D oxide nanostructures

Only for materials with anisotropic crystallographic structure, a 1D growth along one specific crystallographic direction can be obtained by hydrothermal synthesis (assuming equilibrium) as explained in Chapter 2. In most cases and especially for materials with a cubic or pseudocubic crystal structure, 1D directing growth approaches have to be applied. The 1D growth principles that can be used for hydrothermal synthesis are summarized below.

To achieve 1D growth:

- Take advantage of anisotropic crystallographic structure of a solid
- Utilize precursors with 1D nanostructure
- Take advantage of appropriate organic additives (surfactants)
- Use the principle of oriented attachment of non-spherical nanocrystals

The examples to illustrate these growth principles given in the following include; the binary oxides ZnO and TiO_2 as well as complex ferroelectric perovskite-based oxides. ZnO with the anisotropic würtzite structure should in principle grow into 1D structures, TiO_2 grows from very anisotropic titanate precursors while for the cubic or pseudocubic perovskite oxides organic additives are used to aid the 1D nanorod growth.

3.4.1 Hydrothermal growth of 1D nanostuctures of ZnO

This example illustrates that we can take advantage of an anisotropic crystal structure with specific growth in one crystallographic direction. Demonstration of this growth principle for the synthesis of 1D oxide nanostructures is rare in the literature. Zinc oxide (ZnO) is a wide bandgap semiconductor crystallizing in the würzite structure ($P6_3/mc$). Due to the inherent anisotropy in this hexagonal structure, ZnO can be tailored into 1D nanostructures by various methods, but there are only a few reports on ZnO nanostructures by solution-based methods. 1D nanostructures of ZnO are especially attractive due to their tunable electronic and opto-electronic properties and potential applications in optoelectronical devices like light emitting diodes, solar cells and photodetectors, energy harvesting devices, electronic devices, sensors as well as catalysts. 1D nanostructures of ZnO have been prepared by hydrothermal synthesis by several research groups as shown in the review by Baviskar et al.[26] As an example aligned ZnO nanorods (diameter 10-20 nm and length of several μm) have been grown on ZnO film-coated Si substrates by hydrothermal synthesis at 90 °C, see Fig. 4. The precursor was zinc nitrate and hexamethylenetetramine was added. The nanowire diameter could be controlled by the precursor concentration. The ZnO film substrate was covered with many nanocrystallites with a preferred c-axis alignment which served as nucleation centers for the hydrothermal growth of the 1D ZnO nanostructures. The precursor concentration and hence the Zn^{2+}/OH^- ratio at the growth surfaces was found to be important for the formation of the ZnO nanorods which was supposed to occur according to a standard nucleation process.[27]

Room temperature photoluminescence (PL) spectra of as-grown and annealed samples were studied and adsorption and/or desorption of oxygen species from the nanostructure surface was deducted to have a major effect on the PL spectra.

3.4.2 Hydrothermal growth of TiO_2 (anatase via titanate) 1D nanostructures

This example shows how a highly anisotropic crystal structure of an intermediate compound can be transferred into the target oxide TiO_2. TiO_2 is an n-type wide band gap semiconductor with low cost, is non-toxic and has a high stability. TiO_2 is used in a wide variety of applications such as dye-sensitized solar cells, in photocatalysis, and for electrochemical storage. TiO_2 crystallizes in two common crystal structures anatase and rutile, but these phases do not normally grow into 1D nanostructures at hydrothermal conditions. To achieve 1D nanostructures we can take advantage of layered titanate precursor phases like Na-titanate (e.g. $Na_2Ti_5O_{11}$) and K-titanate (e.g. $K_2Ti_6O_{13}$) with highly anisotropic structures which can further be transformed into the 1D nanostructures of anatase.[28] The preparation of 1D nanostructured titanates can be done by a temperature controlled hydrothermal route using TiO_2 as precursor and NaOH or KOH as mineralizer. This hydrothermal process is hence performed at high pH values. The pH and type of any co-solvents (*e.g.* alcohols) used play an important role in controlling the shape and crystal structure of the 1D nanostructured titanate intermediate compound.[29] Furthermore, for example Na-titanate can be turned into H-titanate through an acid exchange with acids like HNO_3, HCl or acetic acid. These metastable 1D H-titanate structures are ideal precursors for the further conversion into anatase nanorods by a heat treatment at about 500 °C. The simplified chemical reactions of the as-prepared materials are illustrated in Eqs. (1) to (3).

$$5\ TiO_2 + 2\ NaOH = Na_2Ti_5O_{11}*H_2O \quad (1)$$

$$Na_2Ti_5O_{11}*H_2O + 2\ HCl = H_2Ti_5O_{11}*H_2O + 2\ NaCl \quad (2)$$

$$H_2Ti_5O_{11}*H_2O = 5\ TiO_2 + 2\ H_2O \quad (3)$$

Thus the final TiO_2 anatase nanostructures are obtained by a three step reaction process: i) the reaction of TiO_2 precursor with alkaline NaOH solution at hydrothermal conditions to form intermediate rod shaped titanate compound, ii) the ion exchange of the intermediate titanate compound to replace Na^+ with H^+ and finally iii) the final calcination to form the target rod shaped compound.

K-titanate can also be transformed into 1D TiO_2 nanostructures through a second hydrothermal synthesis. At present there is an incomplete understanding on the formation mechanism of the 1D TiO_2 nanostructures, but it is most probable that the titanates are formed by a dissolution/reprecipitation mechanism into the highly anisotropic structures for example by a mechanism where nanosheets are exfoliated from the crystalline TiO_2 precursors and combined into the titanates. The different 1D nanostructures that can be formed dependent on the reactions parameters and type og co-solvent are shown in Fig. 5.

Optical absorption and PL studies confirm that the obtained 1D TiO_2 nanostructures possess good crystallinity.[29]

3.4.3 Hydrothermal growth of 1D nanostructures of ferroelectric ternary perovskite-based oxides

This example on perovskite based 1D nanostructures illustrates how directed growth aided by organic additives or oriented attachment of non-spherical nanocrystals can lead to 1D nanostructures. Lead titanate-based materials are state-of-the-art piezo- and ferroelectric materials and for interesting applications such as NEMS, nanophotonics and as energy harvesters 1D nanostructures are necessary. The successful hydrothermal growth of 1D nanostructures of single crystalline multicomponent oxides like the perovskites is not trivial as the perovskite structure whether cubic or pseudo-cubic results typically in equiaxed particles as a strong driving force for growth into 1D structures is not present. Although it has been shown that rod-shaped alkali titanate precursors can be used to form $BaTiO_3$ by a hydrothermal conversion of the precursors together with a Ba precursor in a similar manner as described in Chapter 3.4.2,[21] the application of organic additives (surface absorbing molecules, surfactants) is normally used to direct the growth. The function of the organic additive might be different from case to case and two illustrating examples are given here.

Ferroelectric single crystalline PZT nanowires with diameters from 50 nm up to several hundred nm have been prepared by Wang et al.[30] starting from Pb-nitrate and metal-organic precursors to ensure homogeneous mixing. Polyvinyl alcohol (PVA) was used as a growth directing organic additive. The reaction mechanism for the growth of the 1D nanostructures was reported to follow two stages where the first one included the formation of a tetragonal acicular so-called PX phase (same formula as the perovskite structure with a needle like structure)[30] with fibrous morphology followed by conversion of the PX phase into the target perovskite phase with a similar morphology as illustrated in Fig. 6. The function of the PVA was to direct the growth of 1D nanostructures of the PX phase. In a following topotactic-like transformation the PX phase is converted to a single-crystalline PZT product with the same rod-shaped morphology. Control of the growth conditions for the PX phase, e.g. reaction time, is the key for the growth of perovskite PZT nanowires. Nanoparticles only were obtained doing the same synthesis without the PVA addition. The same route is expected to be used to form other hard and soft PZT-based materials.

In one of our previous works we have described a surfactant-assisted hydrothermal route to produce 1D nanostructures of $PbTiO_3$.[31,32] An amorphous $PbTiO_3$ precursor prepared from a Ti-citrate complex solution and Pb-nitrate together with the surfactant (sodium dodecyl-benzenesulfonate, SDBS) was hydrothermally treated and nanorods with square cross-section of 35-400 nm and length up to 5 mm grew along the [001] direction. The nanorods were either growing out of a microsphere of $PbTiO_3$ nanoparticles making bur-like hierarchical structures or forming hierarchical structures on substrates introduced into the autoclave, see Fig. 7 for examples. The proposed growth mechanism included the formation of crystalline

cube-shaped nanocrystals of $PbTiO_3$ which through oriented aggregation self-assembled into the mesocrystal nanorods. Through a ripening process via dissolution-reprecipitation single crystalline nanorods were formed by elimination of solid–liquid interfaces and the surfactants. The directing force for the self-assembly of the nanocrystals was assumed to be the ferroelectric polarization. The authors demonstrated that the polarization direction in the hydrothermally synthesized $PbTiO_3$ nanorods could be changed from parallel to the nanorod axis to perpendicular to it by a simple heat treatment above the Curie temperature.[33] This control of the polarization in the $PbTiO_3$ nanorods opens up possibilities of tailoring the ferroelectric properties and is therefore highly relevant for the use of ferroelectric nanorods in devices.

This approach has also been followed up by others for instance for the preparation of $(K,Na)NbO_3$ nanorods which were also formed by an oriented assembly mechanism.[34] In synthesis of these kind of multicomponent materials (ternary oxides and higher), where several different phases are present, a modeling of the thermodynamics of the equilibria present taking place in the solutions enables the calculation of stability and yield diagrams giving information about the conditions which should be used for the preparation of a given phase.[22]

4. Molten salt methods of 1D oxide nanostructures

Molten salts are ionic liquids, consisting of anions and cations, which can be stable over a wide temperature range from the melting point up to the boiling point. The ionic nature makes molten salts ideal solvents for oxides, particularly oxides of high valence cations, which can be challenging to dissolve in water or other polar solvents at ambient or under hydrothermal conditions. The solubility of oxides and other precursors in molten salts, combined with the electrical conductivity, good thermal stability and low vapor pressures has made molten salt irreplaceable solvents in electrowinning of metals. Since molten salts are excellent solvents for oxides, molten salt synthesis of complex oxides has become an extremely popular methodology.[12, 35] Recently, also the use of low temperature ionic liquids (low temperature molten salts) has been proposed to be a burgeoning direction on materials synthesis.[36] Although most oxide compounds can be formed using the molten salt method, not all oxides or complex oxides can be synthesized into 1D nanostructures by the molten salt method. In short, the precursor materials and salts are mixed together and heated to a temperature above the melting point of the salt, and the resulting oxide product can be separated from the salt by a simple washing procedure. Due to its easiness the method has been adopted by many researchers, but the simplicity has also lead to many reported synthesis protocols, which apparently give the desired nanomaterials, but which have been shown difficult to reproduce and where fundamental problems can be raised with respect to the proposed mechanism(s).[7] Here, we will first present the principle of the method, discuss possible mechanisms which may give 1D oxide materials, address some concerns with reported reaction mechanism and finally give some examples of successful routes to 1D oxide nanomaterials by using the molten salt method.

4.1 The principles of the molten salt technique

Definition of a molten salt synthesis: A nucleation and growth of an oxide compound in a molten salt solution environment through the dissolution of precursors (oxides, inorganic or organometallic salts/compounds) and precipitation of the oxide product.

The typical synthesis protocol for the molten salt route is illustrated in Fig. 8. The oxide precursor chemistry is rich and may vary from the principle oxides, carbonates, acetates, organometallics or other compounds which will decompose/oxidize to the principle oxide by heating in air. In case of transition metal oxides, the precursor does not necessary have the same oxidation state of the cation in the precursor and in the final product, which means that both reduction and oxidation of the transition metal may take place during the course of the synthesis. The first step is to mix the precursor(s) with the appropriate salt or a mixture of salts, Fig. 7 a). There are several salts available such as chlorides, sulfates, nitrates or hydroxides, etc. The advantage of mixing two salts is that the synthesis temperature can be lowered towards the eutectic temperature of the salt mixture.

In the second step the salt and precursor mixture are placed in a crucible and heated to the desired temperature where the salt becomes molten, Fig. 7 b). The crucible can be closed if water or the amount of oxygen available should be limited, but in case of precursor such as acetates the presence of oxygen is necessary to obtain oxides and the synthesis should be performed in an open crucible. The crucible material may also be critical and refractory oxides and noble metals are good alternatives.

In the third and fourth step at the synthesis temperature, precursor(s) will dissolve into the ionic solvent, and the desired product will first nucleate, Fig. 7 c) and then grow, Fig. 7 d) from the melt due to supersaturation as explained further below. The mechanism(s) of the nucleation and growth and important parameters related to the kinetics of these steps will be elucidated further in Chapter 4.2.

The crucible will finally be cooled to ambient temperature in the fifth step, Fig. 7 e). It has been shown in several studies that the cooling rate is important, which show that the growth might occur also during cooling.

Finally, the salt is removed by washing the product with an aqueous solution in the sixth step shown in Fig. 7 f).

4.2 Mechanism for growth of 1D nanostructures by molten salt method

There are several key issues which need to be addressed in order to understand the nucleation and growth mechanism during molten salt synthesis; i) reactions involved transforming precursors to the principle oxides, ii) solubility of the precursor(s) and the solubility of the desired oxide compound, iii) nucleation kinetics and finally iv) growth kinetics.

i) If the precursors are inorganic or organometallic salts the precursor has to decompose/oxidize to the principle oxide before 1D structures are formed. For example a metal acetate precursor will decompose/oxidize to the metal oxide during heating. Reactions during heating are often neglected, and possible influence of these is thereby also ignored, which may lead to wrong conclusions regarding evaluation of the growth mechanisms. The growth of nanorods of $BaTiO_3$ by adding nonionic surfactants during the mixing the molten salt and precursors was first reported by Mao et al.[37] The decomposition of the organic nonionic surfactants far below the melting point of the salt was not discussed in this first report, and in several following papers the surfactants were claimed to guide the 1D growth due to adsorption of the surfactants at specific crystal facets. The original work on $BaTiO_3$ has been shown to be very difficult to reproduce,[38] demonstrating that both the volatility of the salt and reducing conditions may have a detrimental role for synthesis using these surfactants. The reducing conditions may also enhance the formation of volatile species in halide-rich environments.

ii) The solubility of oxides in molten salt has a wider interest, and there are several examples of investigations, which report on the solubility of principle oxides in some molten salts,[39,40] but in most cases solubility data are not available. Despite the lack of quantitative data, the solubility of binary oxides (*e.g.* $BaTiO_3$) relative to the two principle oxides it is made from (BaO and TiO_2), can be given. If the Gibbs energy of the formation reaction of the binary oxide from the principle oxides is strongly negative, the solubility of the binary oxide is much lower relative to the sum of the two principle oxides. Supersaturation of the complex oxide is therefore obtained when the principle oxide precursors are first dissolving in the molten salt flux. Precursors such as organometallic compounds or metal salts, which form the principle oxide by decomposition/oxidation, will also lead to supersaturation. Since the reaction occurs rapidly due to heating, the principle oxide formed by the decomposition reaction yields a nanocrystalline oxide product with high Gibbs energy due to high surface/interface area and defects, which will enhance the solubility in the molten salt relative to highly crystalline materials. If the bulk target oxide material is used as precursor, supersaturation is not possible and nanostructures will not form since the bulk crystal will have lower Gibbs energy and only grain growth may occur.

iii) Nucleation my take place by homogeneous or heterogeneous nucleation. Homogeneous nucleation is most likely if most of the precursors dissolve in the molten salt, while in cases where one of the precursors or one or several principle oxides have a low solubility, heterogeneous nucleation is most likely. High nucleation rate is advantages for the growth of nanostructures.

iv) A prerequisite for the growth of 1D nanorods is that the growth rate is higher in one specific crystallographic direction. Molten salts do not allow the use of surfactants or other species which may adsorb on specific crystal surfaces due to lack of stability of such compounds under these harsh conditions. Anisotropic crystal growth is therefore only possible due to crystallographic anisotropy, and isotropic cubic crystal structures will form cubes in molten salts. The more anisotropic the structure is the more likely is the formation of 1D nanorods, but anisotropy may also give 2D nanostructures like plates or belts.

4.3 How to perform the molten salt synthesis

Before you decide to use this synthesis method you need to find out if the crystal structure of the compound is anisotropic. If your targeted material has a cubic or pseudocubic crystal structure you have to choose another method like hydrothermal and use the 1D directing growth principles presented in Chapter 2. The molten salt synthesis is quite simple to perform and all you need are the precursors, the salt for the flux, a crucible which does not react with the flux and a high temperature furnace. Start to postulate the overall reaction that will take place in the molten salt environment and look at decomposition of the precursors if they are not oxides. Also evaluate if the precursors may react with the molten salt and for example form volatile compounds that will change the composition of the flux. Thereafter, find an appropriate mixture of molten salt to reduce the reaction temperature or use precursors, which may reduce the melting point of the molten salts. Perform the reaction at the lowest possible temperature to control the diameter of the 1D nanorods. After the cooling, the salt flux has to be washed away and the product collected.

4.4 Molten salt synthesis of 1D oxide nanostructures

Growth principle for molten salt method:

Take advantage of an anisotropic crystal structure.

In the following four examples of the successful synthesis of 1D oxide nanostructures by the molten salt synthesis method will be presented. With this synthesis method the space for playing with growth principles is more limited than for using *e.g.* hydrothermal synthesis and mainly only the growth directing approach fabricating materials with a highly anisotropic crystal structure can be grown. There are indications in the literature that interactions and absorption of specific ions from the molten salt on specific crystallographic faces can tune the growth direction by blocking growth in certain directions. Direct evidence of this mechanism is however still lacking. We will present one example of this in Chapter 4.4.2 where the polar surfaces of ZnO may play a detrimental role by growth of ZnO 1D nanostructures.

4.4.1 Formation of MnO_2 nanorods in two different polymorphs

Sui et al.[41] have reported on the formation of nanorods of two different polymorphs of MnO_2, where none of the polymorphs have a cubic crystal structure. MnO_2 which shows several polymorphs can be applied in areas as catalyst, ion exchange, electrochemical supercapacitor, etc.[41] 1D nanostructures of α-MnO_2, with tetragonal crystal structure (space group *I4/m*, a=9.784 Å, c=2.863), was prepared in molten KNO_3 between 360-400 ºC using the precursor $MnSO_4$. The needles with length of several micrometers and diameter of 15-30 nm were shown to be single crystals growing along the <001> direction. If the solvent (molten salt)

was replaced with a mixture of $NaNO_3$ and $LiNO_3$, nanorods of another polymorph β-MnO_2 were formed at 380 ºC. β-MnO_2 has also a tetragonal crystal structure ($P4_2/mnm$, a = 4.399Å, c=2.874 Å), and also needle like single crystals were formed in this case with somewhat larger diameter (20-40 nm). The 1D nano-crystals were shown to grow along the <002> direction. X-ray diffractograms, TEM and SEM images of the 1D nanorods of α- and β-MnO_2 are displayed in Fig. 9 and 10, respectively.

The precursor $MnSO_4$ used in this synthesis decomposes and oxidizes during the reaction according to reaction (4).

$$MnSO_4 + ½\ O_2(g) = MnO_2 + SO_3(g) \qquad (4)$$

The precursor salt, with Mn(II) has higher solubility in the molten salt compared to the product with oxidation state Mn(IV). The molten salt therefore becomes supersaturated on manganese, which facilitate the formation of the nanorods. Below 360 ºC, no phase pure products could be formed, while above 400 ºC MnO_2 is unstable due to thermal reduction and, and Mn_2O_3 was formed instead.

In both the two molten salts used an amorphous oxide precursor was formed when the precursor was added to the molten salt. The oxidation state of Mn in the amorphous oxide, found in the initial stage of the synthesis, was not investigated. The formation mechanism of α-MnO_2 was suggested to be based on the curling of nanosheets, whereas the formation of the β-MnO_2 nanorods was proposed to go through a heterogeneous nucleation and dissolution-recrystallization process. It is however important to notice that both crystal structures are non-cubic and anisotropic giving reasons to suggest that the growth rate in different crystallographic directions are different, which accelerates the growth in one specific crystallographic direction. Finally, the difference in the size of the cations in the molten salts was suggested to have a stabilizing effect, which means that α-MnO_2 was stabilized by the larger K^+, while β-MnO_2 was stabilized by the smaller Li^+/Na^+.

4.4.2 Molten salt formation of ZnO nanorods

Molten salt synthesis has also been reported for hexagonal ZnO with würtzite structure by Jiang et al.[42] 1D structures of ZnO was prepared in molten LiCl at 615 ºC using the precursor zinc acetate or other precursors like zinc sulfate. Single crystal ZnO nanorods with diameter 30-70 nm and length up to several nanometers were obtained, growing in the <100> and <102> directions. The nanorods were shown to possess a slightly wavy surface along the growth direction, which is not typical for nanorods formed by other techniques as for instance hydrothermal growth as shown in Chapter 3.4.1. The ZnO nanorods are shown in Fig. 11.

The zinc acetate precursor decomposes/oxidizes during the reaction according to reaction (5).

$$Zn(CH_3COO)_2 + 4\ O_2(g) = ZnO + 4\ CO_2(g) + 3\ H_2O(g) \qquad (5)$$

Reaction (5) occurs during heating up to above the melting point of the molten salt (610 ºC), and the zinc oxide formed in the reaction is suggested to have a higher solid solubility relative to the ZnO nanostructures which nucleates and grow during the synthesis. The nucleation and growth kinetics was strongly dependent on the overall amount of zinc precursors, and heterogeneous nucleation or change in growth mode on the ZnO nanorods occurred if the ZnO concentration was higher than 2 wt%, causing tree-like dendrites of ZnO nanocrystals to be formed.

ZnO with the würtzite crystal structure, with all the possoible applications as outlined above, has been shown to grow into ZnO nanorods under hydrothermal conditions as described in Chapter 3.3.1 and by various vapor deposition techniques.[43] The hexagonal and polar crystal structure facilitates the growth along specific directions. In the molten LiCl environments, it was suggested that Li^+ and Cl^- was stronger bonded at the polar surfaces of the ZnO crystals, favoring the growth in the non-polar direction of the würtzite crystal structure. By this approach we see that we can direct the growth in one direction by blocking the growth on the polar surface.[42]

4.4.3 Formation of $Na_2Ti_6O_{13}$ whiskers by molten salt method

High temperature molten salt synthesis of the complex oxide $Na_2Ti_6O_{13}$ with a highly anisotropic monoclinic crystal structure (*C2/m*) has been reported by Teshima et al.[44] The whiskers which are interesting for the use as photocatalysts were synthesized in a NaCl flux below 1100 ºC using Na_2CO_3 and TiO_2 as precursors. The most important processing parameters were the synthesis temperature and the cooling rate. The diameter of the single crystal whiskers were shown to be reduced to 100 nm with rapid cooling from 700 ºC. Even smaller whiskers could be formed at lower temperatures, but in this case the product was not phase pure and contained the TiO_2 precursor material. The crystal structure of $Na_2Ti_6O_{13}$ is strongly anisotropic with edge sharing TiO_6 octahedra connected in such a pattern leading to tunnels filled with Na^+ along the b-axis, and the elongated direction of the whiskers along the <010> direction clearly reflects the anisotropic nature of the crystal structure as can be seen in Fig. 12 together with a SEM image of the $Na_2Ti_6O_{13}$ whiskers grown from the NaCl flux.

$Na_2Ti_6O_{13}$ is formed due to the reaction between the two precursors giving by the overall reaction (6).

$$Na_2CO_3 + 6\ TiO_2 = Na_2Ti_6O_{13} + CO_2(g) \qquad (6)$$

The synthesis was shown to work well below the melting point of NaCl, demonstrating that the molten salt flux is actually the binary molten mixture Na_2CO_3-NaCl (eutectic point at 633 ºC). The volume fraction of the molten flux does therefore change due to formation of $Na_2Ti_6O_{13}$ and removal of Na_2CO_3 from the melt. The presence of TiO_2 precursor below 700 ºC and the effect of rapid cooling demonstrate that the solubility of TiO_2 is an important factor concerning the growth of the whiskers. The 1D growth is caused by the anisotropic nature of the crystal structure, which give enhanced growth rate along the <010> direction.

Like TiO_2 $Na_2Ti_6O_{13}$ 1D nanostructures may have interesting properties with respect to photo-catalysis and water splitting by light.

The formation of whiskers of $Na_2Ti_6O_{13}$ may also take place in cases were 1D nanostructures of other binary oxides containing TiO_2 are the main target.[38] For example if $PbTiO_3$ is synthesized by molten salt method, NaCl may react with the PbO precursor causing loss of $PbCl_2(g)$ leading to formation of $Na_2Ti_6O_{13}$ as shown in equation (7).

$$2\ NaCl + PbO + 6\ TiO_2 = Na_2Ti_6O_{13} + PbCl_2(g) \quad (7)$$

A similar reaction was also suggested in case of syntheses of $BaTiO_3$, where nanorods of $BaTi_2O_5$/$BaTi_5O_{11}$ were observed. The reaction with the molten flux and precursors may also take place through the gas phase since NaCl and other chloride melts has a considerable vapor pressure above the melting point.

4.4.4 Formation of $K_2Nb_2O_{11}$ whiskers

Molten salt synthesis of whiskers of Nb-containing compounds has received increased attention due to the interesting lead-free piezoelectric materials based on niobium oxide. $K_2Nb_2O_{11}$ whiskers have been synthesized using KCl as molten flux at 1000 ºC using K_2CO_3 and Nb_2O_5 as precursors by Madaro et al.[45] Even at temperatures as high as 1000 ºC single crystal whiskers with less than 500 nm diameter and length of several of tenth of micrometers could be obtained, while significantly thinner whiskers could be obtained at lower temperatures although this was not further studied in this investigation. $K_2Nb_2O_{11}$ has a tungsten bronze tetragonal crystal structure (*P4/mbm*) with an anisotropic crystal structure with chains of corner-shearing NbO_6 octahedra along the c-axis. The whiskers were shown to grow along the c-axis, demonstrating the enhanced growth kinetics along perovskite like chains of corner shearing octahedra. An image of the whisker is shown in Fig. 13.

$K_2Nb_2O_{11}$ was formed due to the reaction between the two precursors giving the overall reaction (8).

$$K_2CO_3 + Nb_2O_5 = Na_2Ti_2O_{11} + CO_2(g) \quad (8)$$

In this case the cation of the /precursor/product and the molten salt has a common cation excluding possible contaminations/complications by formation of undesired products.

A similar molten salt route to whiskers of KNb_3O_8, also with a non-cubic anisotropic crystal structure, have been prepared by a similar route using only Nb_2O_5 as precursor and KCl molten salt at 800 ºC.[46] In this case the molten slat flux is consumed during the reaction, leading to the overall reaction (9).

$$5\ KCl + 8\ Nb_2O_5 = 5\ KNb_3O_8 + NbCl_5(g) \quad (9)$$

The KNb_3O_8 nanowires can further be used as precursors to prepare nanowires of other Nb-based oxides. KNb_3O_8 is first transformed to $H_3ONb_3O_8$ nanowires by treatment in nitric acid, and $H_3ONb_3O_8$ is further transformed to Nb_2O_5 nanowires by heat treatment. The Nb_2O_5

nanowires are finally transformed by a second molten salt step to $LiNbO_3$[47] or $KNbO_3$ nanowires. [46] In the final step molten KCl is applied together with Li_2CoO_3 or K_2CO_3 to give the desired product.

5 Conclusions

Synthesis of materials with desired crystal structure, morphology, phase purity and purity in a reproducible and environmental friendly manner has received considerable attention in material science all over the world. Nanotechnology has motivated a tremendous effort in the synthesis approaches to obtain free standing and hierarchical 1D oxide nanostructures. 1D oxide nanostructures can be grown by both physical and chemical synthesis methods and here we have given a tutorial review of formation of 1D oxide nanostructures from chemical solutions. This synthesis approach has several advantages over physical deposition methods or lithographic methods including that they are very simple, is less costly, can easily be up-scaled and that the synthesis parameters like temperature, precursors and concentration in the solution can easily be varied.

Only materials exhibiting an anisotropic crystal structure will grow naturally into 1D nanostructures. For all other crystal structures we need to direct the growth by other means and the principles to control the growth in one direction includes a) utilize a precursor with 1D nanostructure, b) use of appropriate organic additives or surfactants to aid directed growth, c) oriented attachment of non-spherical nanocrystals into 1D nanostructures, d) confinement by a hard template with 1D morphology or e) confinement of a liquid drop.

A critical overview of preparation of 1D oxide nanostructures in solutions with emphasis on hydrothermal and molten salt synthesis has been presented. The main advantage of these methods compared to other wet chemical methods is the increased solubility of the precursors under the conditions of the syntheses. A high solubility is important to achieve a high nucleation rate which is necessary to obtain nanomaterials. Furthermore, the hydrothermal method is very flexible with respect to the possibilities for using 1D directing approaches while in case of the molten salt method it is to a large extent limited to the growth of 1D materials with anisotropic structure. The principles of the methods, thermodynamic and kinetic aspects with respect to nucleation and growth and how to direct growth in one specific direction are elaborated and explained. The importance of synthesis parameters, solubility of precursors, precursor chemistry and the role of organic additives is highlighted and explained. Some guidelines about how to proceed to prepare a new material into 1D nanostructures is presented and illustrated with selected examples from the literature.

The knowledge about e.g. the solubility of different precursors and the understanding of the growth mechanisms of these 1D nanostructures is still not fully determined. Hence a trial and error approach is normally carried out based on established protocols from the literature. Improved understanding of the chemical and physical conditions and the structural aspects of

the materials is called upon to move away from the more common trial and error approach. One can therefore anticipate future promising developments of chemical synthesis of 1D oxide nanostructures as further knowledge and understanding are gained. Focus on lower melting temperature molten salts (ionic liquids) and higher temperature hydrothermal synthesis as new technology for autoclaves is developed is anticipated to be important. In the mean-time the use of thermodynamic data and calculations, combinatorial approaches as well as *in-situ* techniques will guide us to new synthesis protocols.

References

1. Y. Xia, P. Yang, Y. Sun, Y. Wu, B. Mayers, B. Gates, Y. Yin, F. Kim and H. Yan, *Adv. Mater.*, 2003, 15 2003, 353-389.
2. C.N.R. Rao, F.L. Deepak, G. Gundiah and A. Govindaraj, *Progr. Solid State Chem.,* 2003, 31, 5-147.
3. E. Comini, C. Baratto, G. Faglia, M. Ferroni, A. Vomiero and G. Sberveglieri, *Prog. Mater. Sci.,* 2009, 54, 1-67.
4. M.M. Arafat, B. Dinan, S.A. Akbar and A.S.M.A. Haseeb, *Sensors,* 2012, 12, 7207-7258.
5. P. Ayyub, V.R. Palkar, S. Chattopadhyay and M. Multani, *Phys. Rev. B,* 1995, 51, 6135-6138.
6. K.A. Dick, K. Deppert, M.W. Larsson, T. Mårtensson, W. Seifert, L.R. Wallenberg and L. Samuelson, *Nat. Mat.,* 2004, 3, 380-384.
7. P.M. Rørvik, T. Grande and M.-A. Einarsrud, *Adv. Mater.,* 2011, 23, 4007-4034.
8. A.L. Tiano, C. Koenigsmann, A.C. Santulli and S.S. Wong, *ChemComm,* 2010, 46, 8093-8130.
9. Y. Mao, T.-J. Park, F. Zhang, H. Zhou and S.S. Wong, *Small,* 2007, 3, 1122-1139.
10. R. I. Walton, *Chem. Soc. Rev.,* 2002, 31, 230-238.
11. W. Shi, S. Song and H. Zhang, *Chem. Soc. Rev.,* 42, 2013, 5714-5743.
12. K.H. Yoon, Y. S. Cho, D. H. Kang, *J. Mater. Sci.* 1998, 33, 2977-2984.
13. P.M. Rørvik, T. Lyngdal, R. Sæterli, A.T.J. van Helvoort, R. Holmestad, T. Grande and M.-A. Einarsrud, *Inorg. Chem.,* 2008, 47, 3173-3181.
14. U. Schubert and N. Hüsing, *Synthesis of Inorganic Materials*, Wiley-VCH Verlag, Weinheim, Germany, 2000.
15. Y.-P. Fang, A.-W. Xu, R.-Q. Song, H.-X. Zhang, L.-P. You, J.C. Yu and H.-Q. Liu, *J. Am. Chem. Soc.,* 2003, 125, 16025-16034.
16. K. Byrappa and M. Yoshimura, *Handbook of hydrothermal technology*, Elsevier, Oxford, UK, 2013.
17. A. Rabenau, *Angew. Chem. Int. Ed.,* 1985, 24, 1026-1040.
18. G. Demazeau, *J. Mater. Chem.,* 1999, 9, 15-18.
19. A.A. Peterson, F. Vogel, R.P. Lachange, M. Fröling, M.J. Antal, J.W. Tester, *Energy Environ. Sci.,* 2008, 1, 32-65.
20. H. Hayashi and Y. Hakuta, *Materials,* 2010, 3, 3794-3817.
21. D.R. Modeshia and R.I. Walton, *Chem. Soc. Rev.,* 2010, 39, 4303-4325.

22. C. Mossaad, M. Starr, S. Patil, R. Riman, *Chem. Mater.,* 2009, 22, 36-46.
23. R. Wendelbo, D.E. Akporiaye, A. Karlsson, M. Plassen and A. Olafsen, *J. Eur. Cer. Soc.,* 2006, 26, 849-859.
24. J.R. Eltzholtz, C. Tyrsted, K.M.Ø. Jensen, M. Bremholm, M. Christensen, J. Becker-Christensen, B.B. Iversen, *Nanoscale,* 2013, 5, 2372-2378.
25. T. Adschiri, K. Kanazawa and K. Arai, *J. Am. Cer. Soc.,* 1992, 75, 1019-1022.
26. P.K. Baviskar, P.R. Nikam, S.S. Garote, A. Ennaoui and B.R. Sankapal, *J. Alloys Comp.,* 2013, 551, 233-242.
27. Y. Sun, G. Ndifor-Angwafor, D. J. Riley and M.N.R. Ashfold, *Chem. Phys. Lett.,* 2006, 431, 352-357.
28. D.S. Xu, J.M. Li, Y.X. Yu and J.J. Li, *Sci. China Chem.*, 2012, 55, 2334-2345.
29. B. Santara and P.K. Giri, *Mat. Chem. Phys.,* 2013, 137, 928-936.
30. J. Wang, A. Durussel, C.S. Sandu, M.G. Sahini, Z. He and N. Setter, *J. Crystal Growth,* 2012, 347, 1-6.
31. G. Wang, R. Sæterli, P. M. Rørvik, A. T. J. van Helvoort, R. Holmestad, T. Grande and M.-A. Einarsrud, *Chem. Mater.,* 2007, 19, 2213-2221.
32. P.-M. Rørvik, T. Grande, and M.-A. Einarsrud, *J. Crystal Growth Design,* 2009, 9, 1979-1984.
33. R. Säterli, P.M. Rörvik, C.C. You, R. Holmestad, T. Tybell, T. Grande, A.T.J. van Helvoort, M.-A. Einarsrud, *J. Appl. Phys.,* 2010, 108, 124320-124326.
34. Y. Xu, Q. Yu and J.-F. Li, *J. Mater. Chem.,* 2012, 22, 23221-23226.
35. M. Bharathy and H.C. zur Loye, *J. Solid State Chem.,* 2008, 181, 2789-2795.
36. Z. Ma, J. Yu and S. Dai, *Adv. Mater.,* 2010, 22, 261-285.
37. Y. Mao, S. Banerjee, S.S. Wong, *J. Am. Chem. Soc.,* 2003, 125, 15718-15719.
38. P.M. Rørvik, T. Lyngdal, R. Sæterli T. Grande, A.T.J. van Helvoort, R. Holmestad, M.-A. Einarsrud, *Inorg. Chem.*, 2008, 47, 3173-3181.
39. V.L. Cherginets, E.G. Klailova, *Electrochim. Acta*, 1994, 39, 823-829,
40. T. Ishitsuka, K. Nose, *Corr. Sci.,* 2002, 44, 247-263.
41. N. Sui, Y. Duan, Jiao, D. Chen, *J. Phys. Chem. C*, 2009, 113, 8560-8565.
42. Z.-Y. Jiang, T. Xu, Z.-X. Xie, Z.-W. Lin, X. Zhou, X. Xu, E.-B. Huang, L.-S. Zheng, *J. Phys. Chem. B*, 2005, 109, 23269-23273.
43. A.B. Djurisic, X. Chen, Y.H. Leung and A.M.C. Ng, *J. Mater. Chem.,* 2012, 22, 6526-6535.
44. K. Teshima, S.H. Lee, S. Murakoshi, S. Suzuki, K. Yubuta, T. Shishido, M. Endo, S. Oishi, *Eur. J. Inorg. Chem.,* 2010, 2936-2940.
45. F. Madaro, R. Sæterli, J.R. Tolchard, M.-A. Einarsrud, R. Holmestad, T. Grande, *CrystEngComm,* 2011, 11, 1304-1313.
46. L. L, J. Deng, J.Chen, X. Sun, R. Yu, G. Liu, X. Xing, *Chem Mater.,* 2009, 21, 1207-1213.
47. L. L, J. Deng, J. Chen, X. Sun, R. Yu, G. Liu, X. Xing, *CrystEngComm,* 2010, 12, 2675-2678.

Figure captions

Fig. 1 Density, dielectric constant and ionic product, K_w, of water at 30 MPa as a function of temperature. Reproduced from Ref. 19.

Fig. 2 Pressure - temperature dependence of water for different degrees of filling of the autoclave during hydrothermal synthesis. Reproduced from Ref. 10.

Fig. 3 A schematic of a Teflon® lined stainless steel autoclave typically used for hydrothermal synthesis. Reproduced from Ref. 10.

Fig. 4 a) TEM image of ZnO nanorods and SEM image of ZnO nanorods grown on a ZnO-covered Si-substrate grown hydrothermally from zinc nitrate for 9 h. Reprinted with permission from Ref. 27. Copyright 2006 Elsevier.

Fig. 5. Schematic of the growth mechanism of different 1D titanate and TiO_2 nanostructures formed at different temperatures using various solvents. Reprinted with permission from Ref. 29. Copyright 2013 Elsevier.

Fig. 6 Scheme of the proposed growth mechanism for PZT nanorods. Reprinted with permission from Ref. 30. Copyright 2012 Elsevier.

Fig. 7 $PbTiO_3$ nanorods and hierarchical 1D nanostructures growth by oriented attachment of cube-shaped $PbTiO_3$ nanocrystals. Images courtesy of Dr. Per Martin Rørvik.

Fig. 8 Illustration of the protocol for molten salt synthesis.

Fig. 9 1D nanostructures of β-MnO_2 formed by the molten salt synthesis in $LiNO_3/NaNO_3$ using $MnSO_4$ as precursor. Reprinted with permission from Ref. 41. Copyright 2009 American Chemical Society.

Fig. 10 1D nanostructures of β-MnO_2 formed by the molten salt synthesis in $LiNO_3/NaNO_3$ using $MnSO_4$ as precursor. Reprinted with permission from Ref. 41. Copyright 2009 American Chemical Society.

Fig. 11 X-ray diffraction pattern and TEM images of ZnO nanorods grown using Zn-acetate as the precursor and LiCl as the molten salt flux. The wavy surface along the growth direction is clearly seen from the HRTEM image. Reprinted with permission from Ref. 42. Copyright 2005 American Chemical Society.

Fig. 12 Schematic representation of the $Na_2Ti_6O_{13}$ structure (a) and SEM image of typical $Na_2Ti_6O_{13}$ whiskers grown at 1100 °C using a cooling method with a NaCl flux. Reprinted with permission from Ref. 44. Copyright 2010 Wiley.

Fig. 13 TEM images a) and b), SAED pattern taken from the zone axis [010] from the red square in a) and projection of the tetragonal tungsten-bronze crystal structure on the (001) plane. Reproduced from Ref. 45.

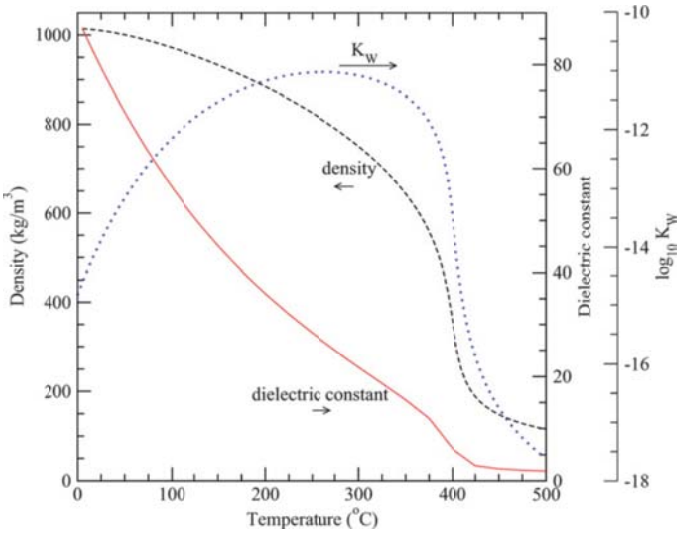

Fig. 1 Density, dielectric constant and ionic product, K_w, of water at 30 MPa as a function of temperature. Reproduced from Ref. 19.

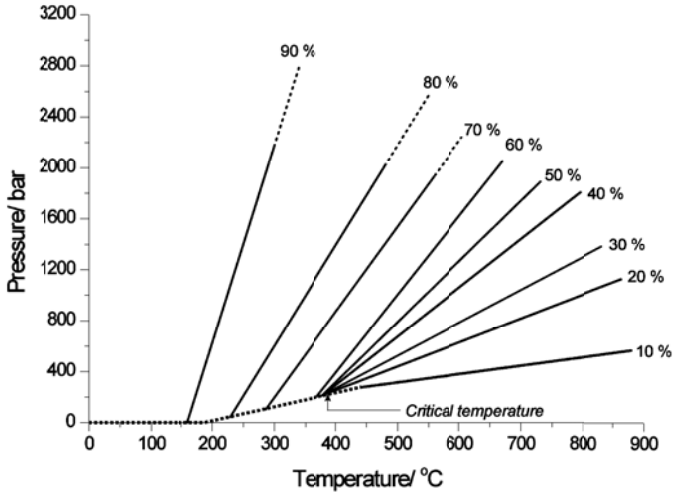

Fig. 2 Pressure - temperature dependence of water for different degrees of filling of the autoclave during hydrothermal synthesis. Reproduced from Ref. 10.

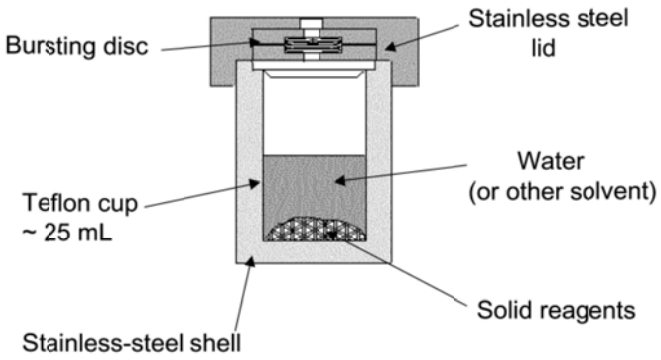

Fig. 3 A schematic of a Teflon® lined stainless steel autoclave typically used for hydrothermal synthesis. Reproduced from Ref. 10.

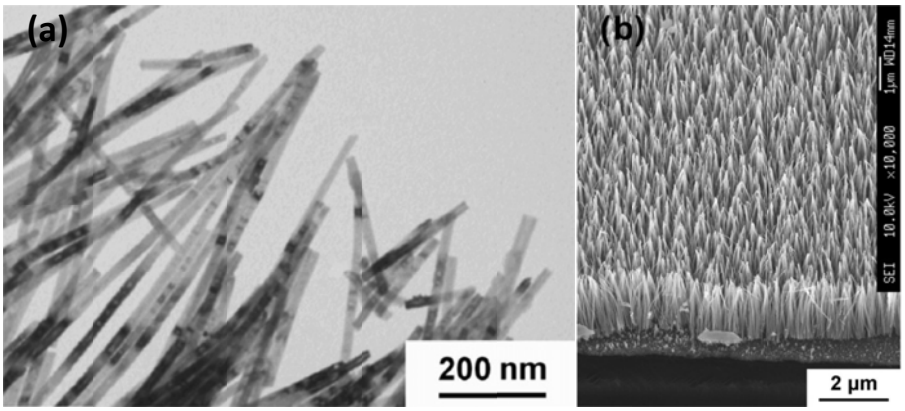

Fig. 4 a) TEM image of ZnO nanorods and b) SEM image of ZnO nanorods grown on a ZnO-covered Si-substrate grown hydrothermally from zinc nitrate for 9 h. Reprinted with permission from Ref. 27. Copyright 2006 Elsevier.

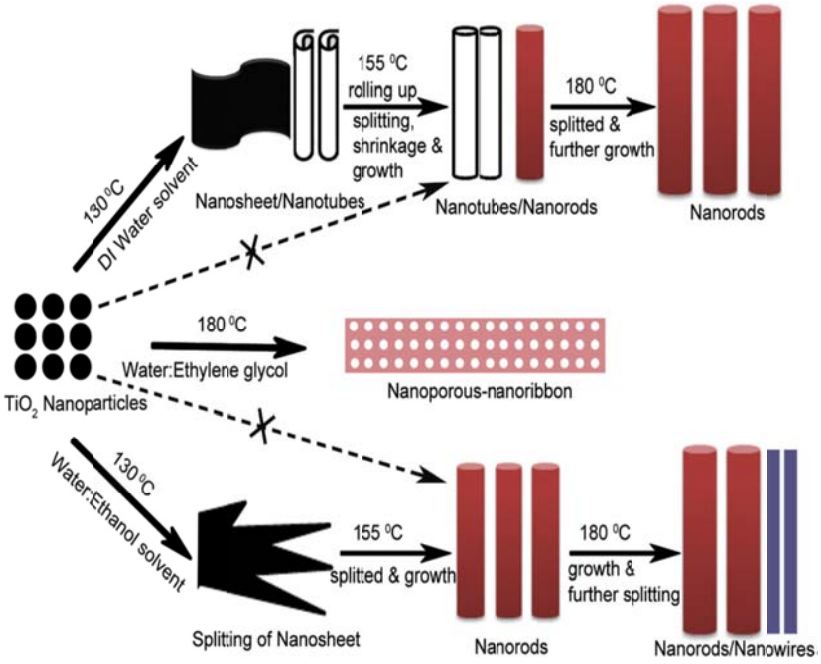

Fig. 5. Schematic of the growth mechanism of different 1D titanate and TiO_2 nanostructures formed at different temperatures using various solvents. Reprinted with permission from Ref. 29. Copyright 2013 Elsevier.

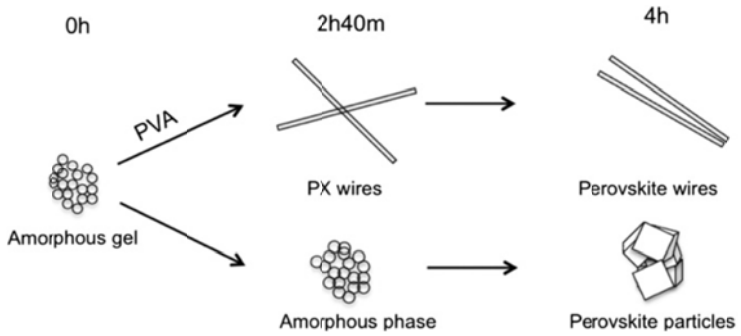

Fig. 6 Scheme of the proposed growth mechanism for PZT nanorods. Reprinted with permission from Ref. 30. Copyright 2012 Elsevier.

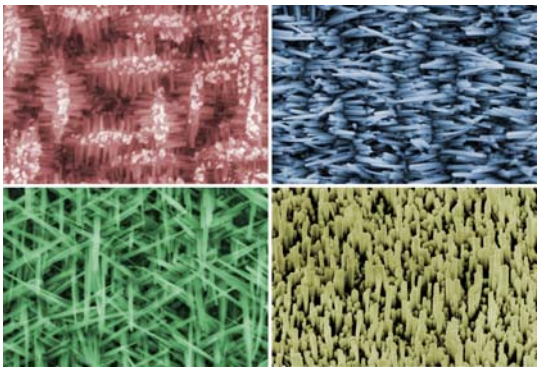

Fig. 7 $PbTiO_3$ nanorods and hierarchical 1D nanostructures growth by oriented attachment of cube-shaped $PbTiO_3$ nanocrystals. Images courtesy of Dr. Per Martin Rørvik.

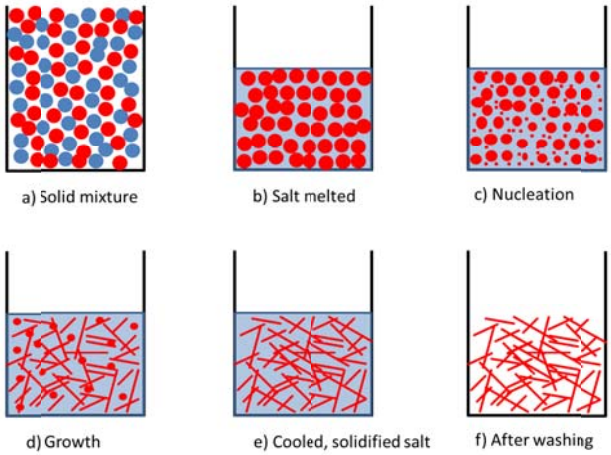

Fig. 8 Illustration of the protocol for molten salt synthesis.

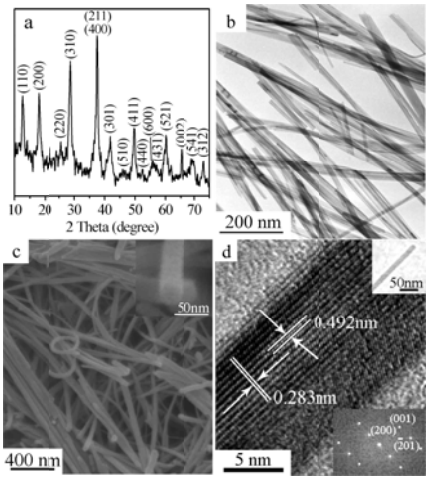

Fig. 9 1D nanostructures of α-MnO_2 formed by the molten salt synthesis in KNO_3 using $MnSO_4$ as precursor. a) XRD pattern, b) TEM, c) SEM and d) HRTEM images. Reprinted with permission from Ref. 41. Copyright 2009 American Chemical Society.

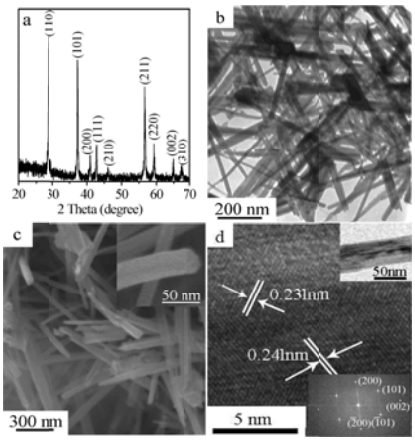

Fig. 10 1D nanostructures of β-MnO_2 formed by the molten salt synthesis in $LiNO_3$/$NaNO_3$ using $MnSO_4$ as precursor. a) XRD pattern, b) SEM, c) TEM and d) HRTEM images. Reprinted with permission from Ref. 41. Copyright 2009 American Chemical Society.

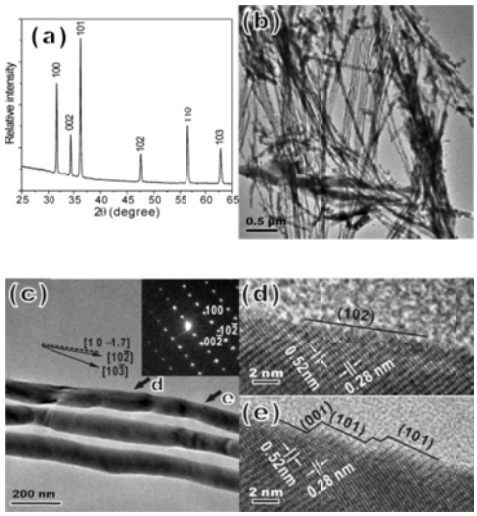

Fig. 11 X-ray diffraction pattern and TEM images of ZnO nanorods grown using Zn-acetate as the precursor and LiCl as the molten salt flux. The wavy surface along the growth direction is clearly seen from the HRTEM image. Reprinted with permission from Ref. 42. Copyright 2005 American Chemical Society.

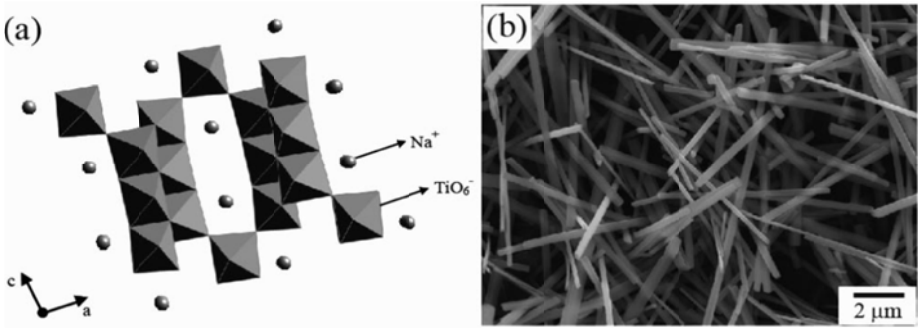

Fig. 12 a) Schematic representation of the $Na_2Ti_6O_{13}$ structure and b) SEM image of typical $Na_2Ti_6O_{13}$ whiskers grown at 1100 °C using a cooling method with a NaCl flux. Reprinted with permission from Ref. 44. Copyright 2010 Wiley.

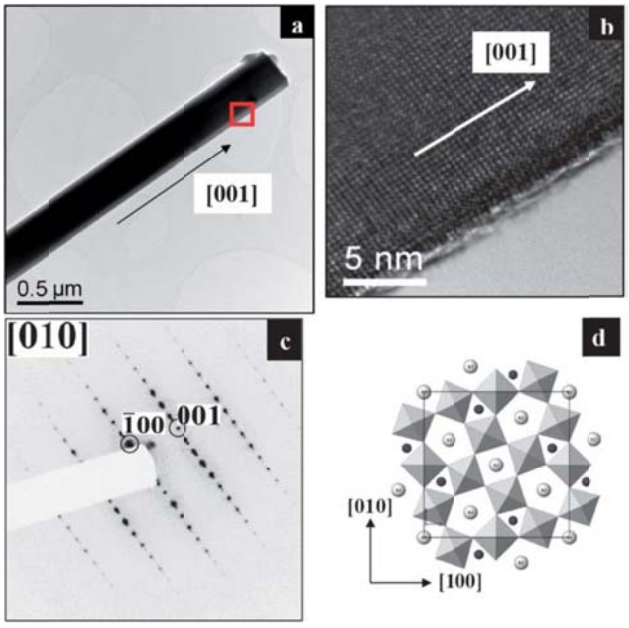

Fig. 13 a) and b)TEM images, c) SAED pattern taken from the zone axis [010] from the red square in a) and d) projection of the tetragonal tungsten-bronze crystal structure on the (001) plane. Reproduced from Ref. 45.